SLAC-PUB-2359
PEP-Note 312
July 1979
(A)

SYNCHRONOUS DETECTION OF BEAM INDUCED PULSES*

J.-L. Pellegrin
Stanford Linear Accelerator Center
Stanford University, Stanford, California 94305

"La nature agit par progrès, *itus et reditus*. Elle passe et revient, puis va plus loin, puis deux fois moins, puis plus que jamais, etc..." - Pascal

This note describes a type of detector which will be used for measuring the amplitudes of short beam induced pulses such as the ones received from a small pick-up electrode. The circuit is called "synchronous" [1] because it takes a sample of the quantity to be measured in synchronism with the pulse repetition rate; the data can be averaged over many samples such as is done for the measurement of the beam position, or the detector output can be observed directly, without any filtering, as is the case when bunch oscillations are sought.

Emphasis was put on three areas in this design: linearity, large dynamic range and immunity to timing variations. Linearily and absence of "knee", or dead zone near the origin, is important for beam position monitoring since they influence the normalization factor; the input-output characteristic of this circuit departs from a straight line by less than 1% of full-scale over four decades of input signal variation. The timing of the detector trigger can change by ± 2 nsec without impairing the above specifications.

(Submitted for Publication)

---

*Work supported by the Department of Energy under contract number DE-AC03-76SF00515

1. Introduction

The pulses induced by the beams into a small electrode (an electrode comparable in size to the bunch length, or smaller) can be either a reproduction of the beam shape when the electrode is loaded by a large impedance, or assumes the form of the derivative of the beam shape whenever the electrode-load time constant is smaller than the bunch length. In any case, the pulse train obtained has no DC component, since the beam pipe current does not carry and DC component, and actually the task of this detector consists in restoring a DC component, linearly related to the pulse peak amplitude. The most straightforward method would be taking directly a sample of the pulse; however, the PEP bunches can be as narrow as 130 psec FWHM, and this approach requires extremely stable, jitter-free triggers. Another method can be sampling a given harmonic of the pulse spectrum, after selective filtering, picking for this component a frequency not too high, yet high enough to yield a large signal-to-noise ratio. The contribution of each beam is then retrieved by sampling the sine wave at different phases, each phase corresponding to the time a bunch traverses the monitor. This solution is elegant but quite impractical because of the difficulty in picking the right frequency harmonic; indeed, if the contribution of each beam is to be reliably sorted out, the two beams' contributions should produce components 90^{o} out of phase with each other, or say $90^{o} \pm 30^{o}$, at the chosen frequency, and this must hold for the signals of any station around the machine. For instance, if one detects the 36th harmonic of the revolution frequency, both beams contribute to it with a phase difference within the above requirements anywhere around the ring except at the stations located at

57.9 and 181.3 meters from the interaction point, where they contribute to this harmonic with a phase difference of less than 25^{o} and therefore do not meet our criterion.

The design described here hinges on an active integrator which linearly stretches the pulse up to 20 ns and allows sampling of its peak without imposing too stringent trigger requirements. Figure 1 is a schematic diagram of the detector.

2. Minimum Beam Induced Pulse

Laboratory tests indicate that the sensitivity to beam current of most Position Monitor electrodes (some electrodes are colser to the beam than others), is of the order of ±3 volts peak per peak ampere, for a bunch length 2σ of 4 cm. It was also experimentally verified that this figure is inversely proportional to σ; since for a given average current the bunch peak current varies also as the reciprocal of σ, we conclude that the electrode beam induced voltage is inversely proportional to σ^2.

In designing this detector, the following assumptions were made regarding the minimum stored beam signal to be expected:

- σ could be as long as twice the nominal value.
- the minimum stored beam for which an orbit measurement is desirable can be as small as 0.25 mA average per bunch.
- as much as 800 ft. of Heliax cable (7/8 inch) is required to reach the detector, and 9 coaxial relays are inserted along this path.

The first two assumptions lead to a minimum peak current of 2.75 A per bunch, and a corresponding electrode voltage of ±8.25 volts.

The coaxial relays' insertion loss amounts to 2.7 dB and the cable loss for this pulse width is of the order of 16 dB; our worst case minimum signal at the detector input becomes ±0.96 Volts. In addition, the transmission line will produce some stretching and we believe that the narrowest pulse received in the control room will measure 0.35 nsec between the positive and the negative peak. The simulation of such a pulse is illustrated in Figure 2: the sharp transition of a snap diode is filtered and produces a narrow, monopolar pulse; the differentiation of this pulse yields the waveform which has been used for testing the synchronous detector.

3. Low Pass Filter

The spectrum of the above typical beam pulse has its maximum amplitude around 1 GHz. It is necessary to remove from this spectrum all the frequencies which would produce a non-linear operation of the integrator; it has been experimentally found that 100 feet of RG196 coaxial cable made an excellent low pass filter. The filter characteristic[2] is plotted on Figure 3 along with a photograph of the response to the minimum, typical beam pulse.

4. Gated Integrator

The reason for gating the integrator is twofold: i) discharge and reset the storage capacitor to avoid accumulation of unwanted charge prior to the beam pulse time of arrival, and ii) separate the contribution of different bunches. Returning to Figure 1, the integrator is seen to be made of two back-to-back current sources having their output clamped to ground by means of a diode switch SW1. The match of the two current

sources is critical; indeed, as the switch opens up, few nanoseconds before beam time, any current unbalance at the source's node will be integrated by C 1 and produce an offset in the detector response. The design of the current sources (Figure 4) is an extension of the design described in Reference 3; the source output current is determined by resistors R 1 , R 3 and R 4 and is the mirror of the current flowing in R 2 . This mirror arrangement provides compensation for the base-emitter junction voltage variation of transitor 3; in addition, transistors 1 and 4 exhibit temperature coefficients with different signs, since transitor 4 has its base-emitter junction connected as a zener diode. The equilibrium of this mirror circuit requires that transitors 3 and 2 have same base currents, so a dual transistor was picked for this pair as well as for transistors 1 and 4 which should be kept at the same temperature. Between 20°C and 60°C a 1 mA source implemented in this fashion was found to have a temperature coefficient of the order of 20 ppm/°C. Figure 5 is a complete integrator diagram. The integrating capacitor is permanently clamped to ground by the diode switch, except in presence of a gate. Two adjustments allow the minimization of the current sources' unbalance and of the gate feedthrough. The typical residual offset is of the order of 1 mV or less, and the maximum integrator output is ±4 volts. Figure 6 represents three input-output waveforms. Integration of the pulse backswing yields the largest output because in this case the gate switch does not divert any current. Yet any of the three outputs can be used for our measurement and one can choose to trigger the sample-and-hold either on the positive or on the negative integrator output; as far as linearity or trigger variation

effects are concerned, no difference could be found between the two methods. On Figure 6, the gate width has been made 50 nsec for the purpose of exploring the integrator waveforms, but for normal operation 30 nsec is acceptable and is sufficient for distinguishing the contribution of two beams at a distance of 5 m from the interaction point.

5. Sampler

A circuit diagram for the sample-and-hold is shown in Figure 7. This type of fast acquisition sampler is used in the design of sampling oscilloscopes[4] or time stretchers.[5] During the short time the diode bridge is turned "on", the storage capacitor charges to a level which represents a fraction only of the input waveform. Between two consecutive sampling times, the capacitor finishes charging by means of the positive feedback applied through the bridge back resistance. The proper adjustment of the loop gain allows to obtain 100% sampling efficiency. Filtering of the sampler output can then be tailored to particular applications; for the case of the position monitors a 7 Hz low pass filter yields an output which reaches one-thousandth of the input after 0.2 seconds.

6. Test Results

The detector sensitivity to trigger variations is shown on Figure 8 where linearity curves have been plotted for signals lower than our minimum beam pulse, with timing varying above and below the optimum timing. For ± 2 nsec variations, which is considerably larger than the trigger system expected variations anywhere around the ring, the detector output drops by about 10%.

A complete detector input-output characteristic has been measured with the set-up of Figure 9; a larger, slower pulse (see inlaid photograph) has been substituted to our test pulse so that the maximum output could be reached. Figure 10 is a log-log plot of the response; its departure from linearity does not exceed 0.7% of full scale.* This data was taken at laboratory temperature. Between 20°C and 60°C, a temperature coefficient of +1 mV/°C was recorded; 80% of this effect was imputed to the voltage follower BB3553 input drift (Figure 5). Most of this residual offset variation has been eliminated by connecting the grounded terminal of the gate bridge to a voltage source of 0 volts with adjustable, negative temperature coefficient; two or three temperature cyclings of the detector allow the adjustment of the compensation voltage source and result in an overall temperature coefficient smaller than ±0.1 mV/°C. Yet this fine zeroing of the detector offset is not absolutely necessary since it is a long term effect that computers can readily subtract, as long as the circuit is linear. More important is the short term stability of the detector output as it comes about in the measurement of the vertical dispersion function.[6] The conventional method requires consecutively plotting beam orbits at different energies, and one finds that the error on the measurement of Eta (y) is equal to the error on the beam position measurement divided by the relative energy variation. Over the time necessary to complete this measurement the detector output is certainly stable to better than 1 part in 2000, and this figure can be improved upon if we use a digital voltmeter instead of the scanning A to

*This figure is questionable since the attenuators of our test set-up are a combination of HP 355C and HP355D with a precision of the order of 1%.

D's as a computer interface. Let us assume that each position monitor electrode measurement a, b c and d involves an rms error of 0.05%; since the vertical beam position is obtained by the combination

$$\Delta y = (18 \text{ mm}) \frac{a - b + c - d}{a + b + c + d}$$

the rms error on Δy will be 0.0045 mm. With an energy variation of 0.002, the error on the measurement of Eta (y) will not exceed 2.25 mm.

7. Conclusion

The beam pulse detector presented here is flexible enough in design to accommodate the normal trigger variations that can be expected on PEP, the current dynamic range and the requirement for measuring the amplitude of any bunch pulse in each beam. The linearity of response of this detector is quite sufficient to monitor the beam positions within 0.1 mm, for bunch average currents between 0.25 and 20 mA, and its stability should allow us to measure Eta (y) values of 1 cm with an error of 25%. Several ways exist for improving on this figure; decision will be made after the first experimental data have been analyzed.

Twelve such detectors have been built for PEP, for reading simultaneously the position of the two beams, along the six sextants of the machine.

References

1. J. D. W. Abernethy, "Box Car Detectors," Research/Development pp. 24-28, June 1971. Other names exist for this type of detector; in particular, Princeton Applied Research seems to have coined the name "Lock-In Amplifier". The detecting element is sometimes a mixer instead of a sampler, but in both cases the equivalent noise bandwidth can be made very small.

2. Data from RF Transmission Line Handbook, Times Wire and Cable Co. Catalog No. TL-5, 1972.

3. G. R. Wilson, "A Monolithic Function FET-NPN Operational Amplifier," IEEE Journal of Solid State Circuits, pp. 341-348, December 1968.

4. J. Mulvey, "Sampling Oscilloscope Circuits," Tektronix publication number 062-1172-00, March 1970.

5. Hewlett-Packard Vector Voltmeter 8405A Operation Manual.

6. M. Cornacchia, M. Lee and J.-L. Pellegrin, "Some considerations of Eta (y) Measurement," PEP-Note 142, March 1978.

Figure Captions

1. Block Diagram of the Synchronous Detector.

2. a) Test pulse generator output, 2 V/div., 0.2 nsec/div.

   b) Response of differentiator (c) to the generator signal, same scale.

   c) Differentiator circuit.

3. Low pass filter characteristic and its response to the typical minimum beam induced pulse after amplification by a cascade of Anzac amplifiers AM117 . AM117 . AM136.

4. Circuit of a current source.

5. Complete circuit of the gated integrator.

6. Three integrator output waveforms for different gate position with respect to the beam pulse; 50 mV/div., 10 nsec/div.

   a) integration of the pulse back swing.

   b) integration of both forward and back swing.

   c) integration of forward swing only.

7. Circuit diagram of the sample-and-hold; the dotted lines represent the feedback path.

8. Detector response to the minimum pulse of Figure 3 with trigger variations as a parameter. Integration and sampling are done on the forward swing.

9. Waveform and set-up used for the measurement of the detector characteristic.

10. Detector characteristic. Integration and sampling are done on the pulse forward swing.

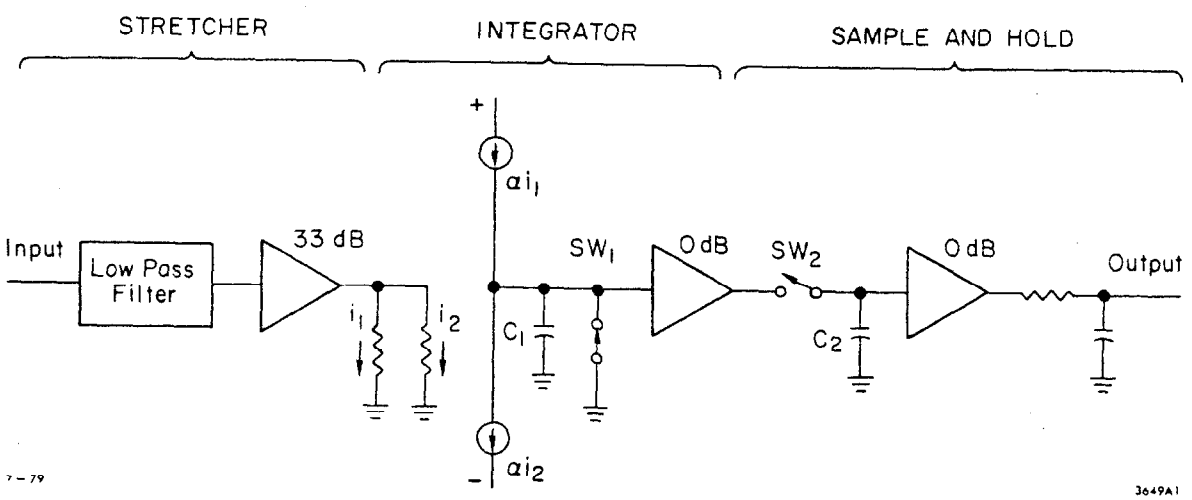
STRETCHER
INTEGRATOR
SAMPLE AND HOLD
Input
Low Pass Filter
33 dB
i_1
i_2
+
αi_1
SW_1
C_1
0 dB
SW_2
C_2
0 dB
Output
αi_2
-
7-79
3649A1

Fig. 1

(a)

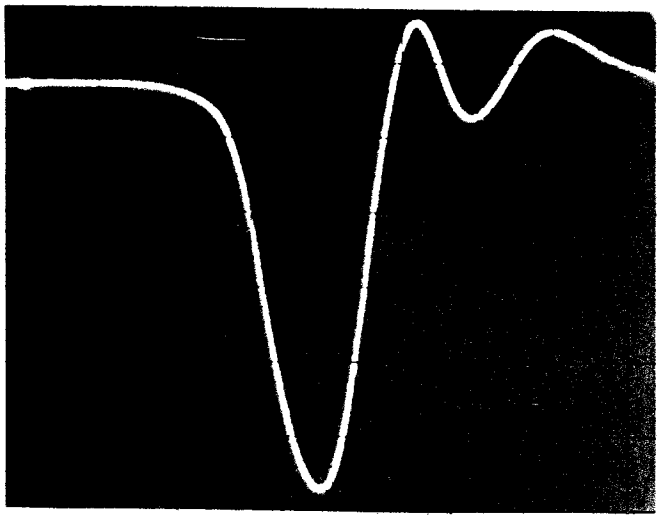

(b)

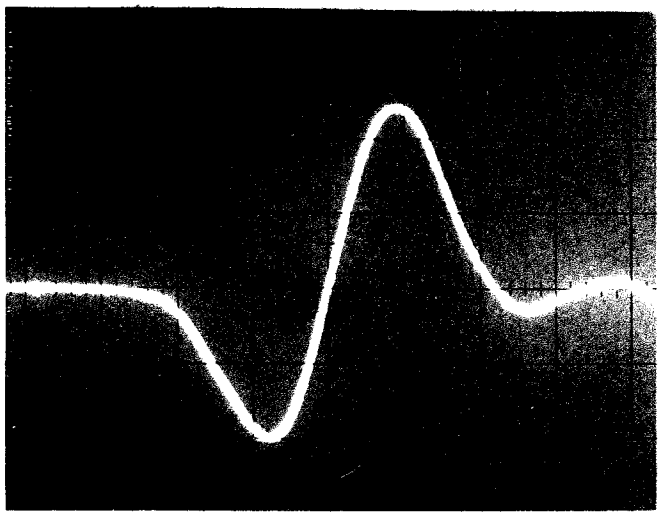

(c)

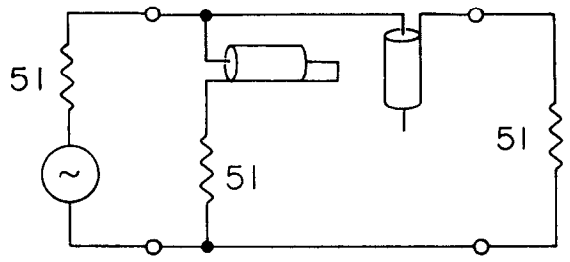

7-79
3649A2 Both stubs are 3 cm of RG196 cable

Fig. 2

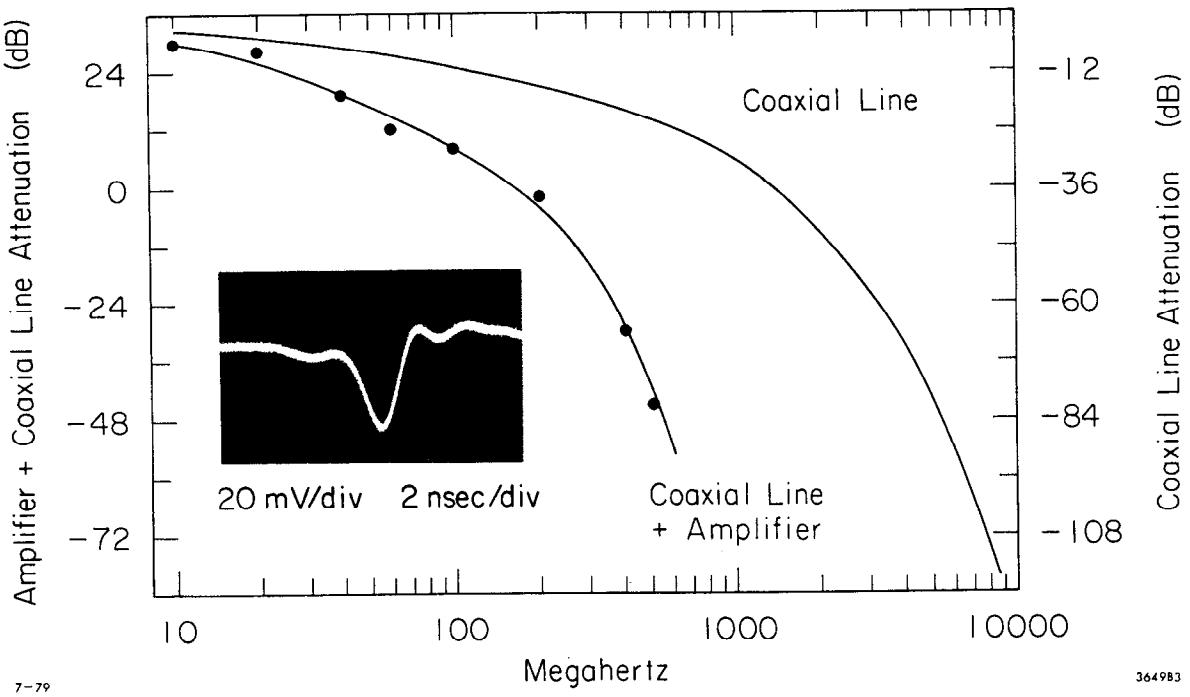
Amplifier + Coaxial Line Attenuation (dB)
24
0
-24
-48
-72
-12
-36
-60
-84
-108
Coaxial Line Attenuation (dB)
Coaxial Line
20 mV/div 2 nsec/div
Coaxial Line
+ Amplifier
10
100
1000
10000
Megahertz
7-79
364983

Fig. 3

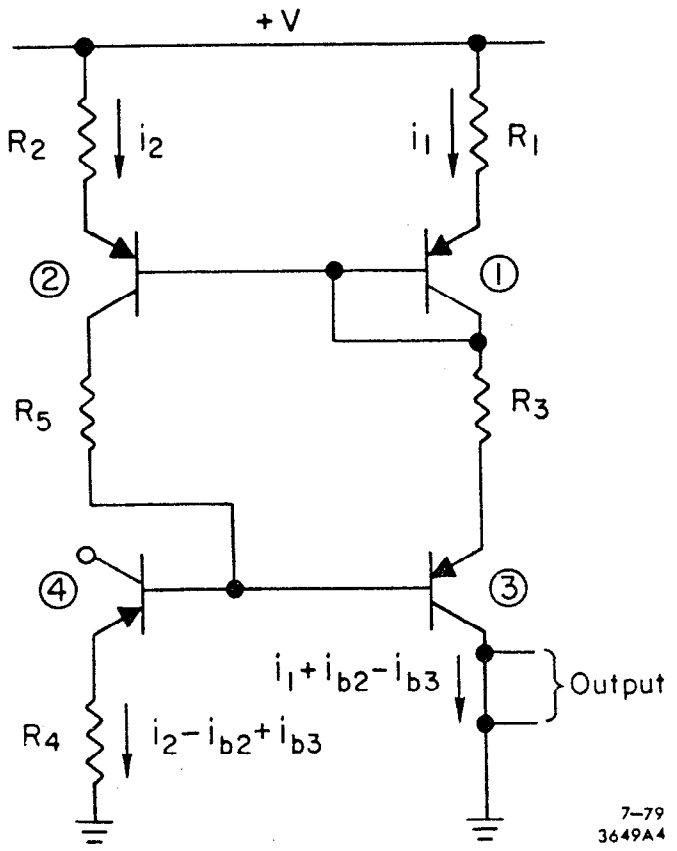
+V
R2
i2
i1
R1
②
①
R5
R3
④
③
i1+ib2-ib3
Output
R4
i2-ib2+ib3
7-79
3649A4

Fig. 4

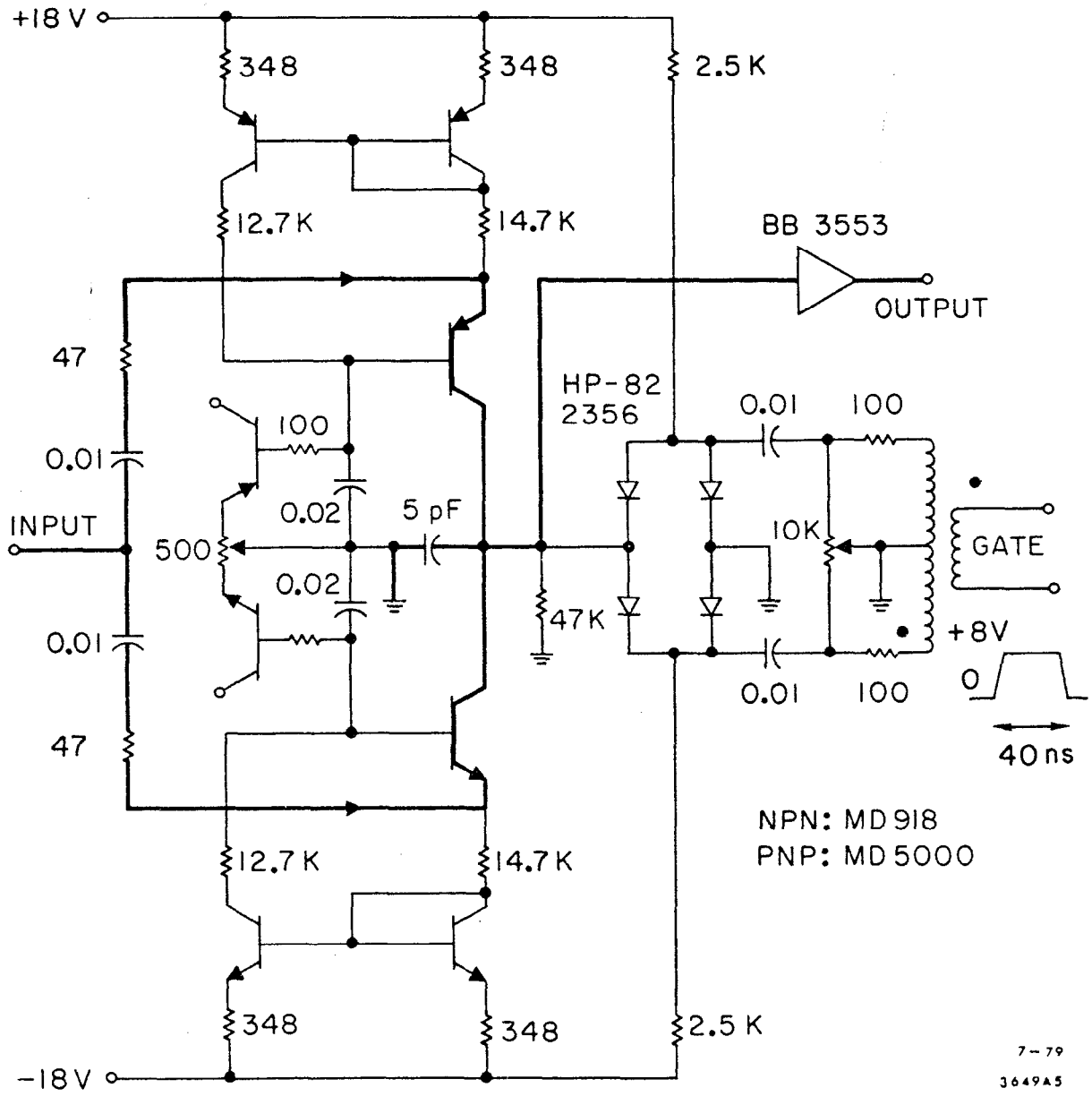
+18 V
348
348
2.5 K
12.7 K
14.7 K
BB 3553
OUTPUT
47
HP-82
2356
0.01
100
0.01
INPUT
0.02
5 pF
500
10K
GATE
0.02
47K
0.01
+8V
0
0.01
100
47
40 ns
NPN: MD 918
PNP: MD 5000
12.7 K
14.7 K
348
348
2.5 K
-18 V
7-79
3649A5

Fig. 5

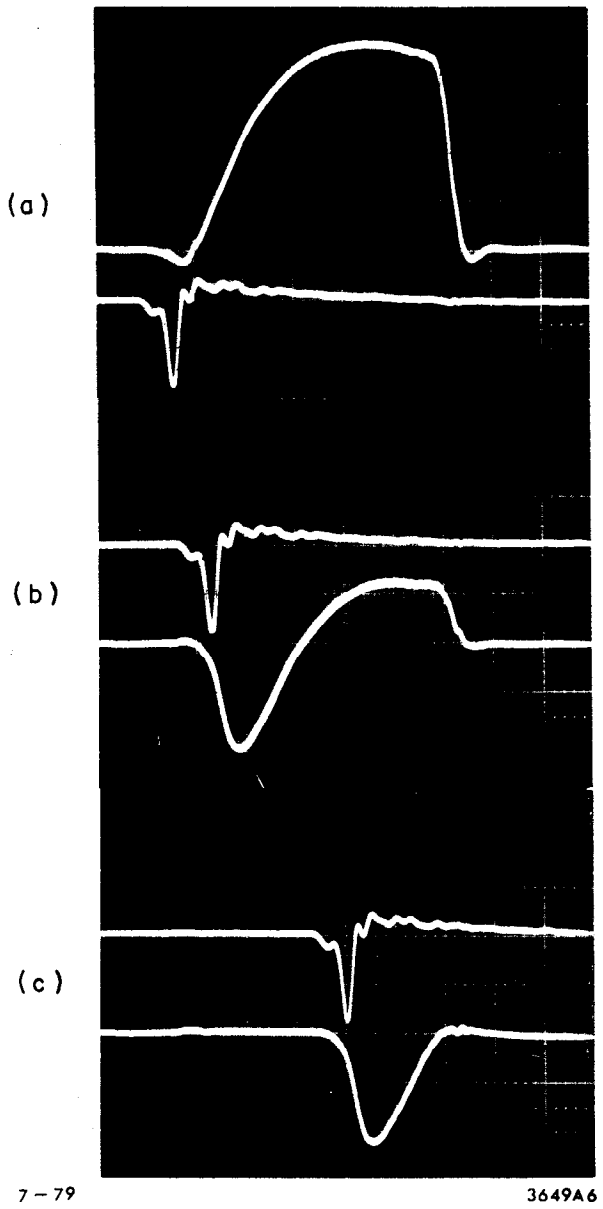

Fig. 6

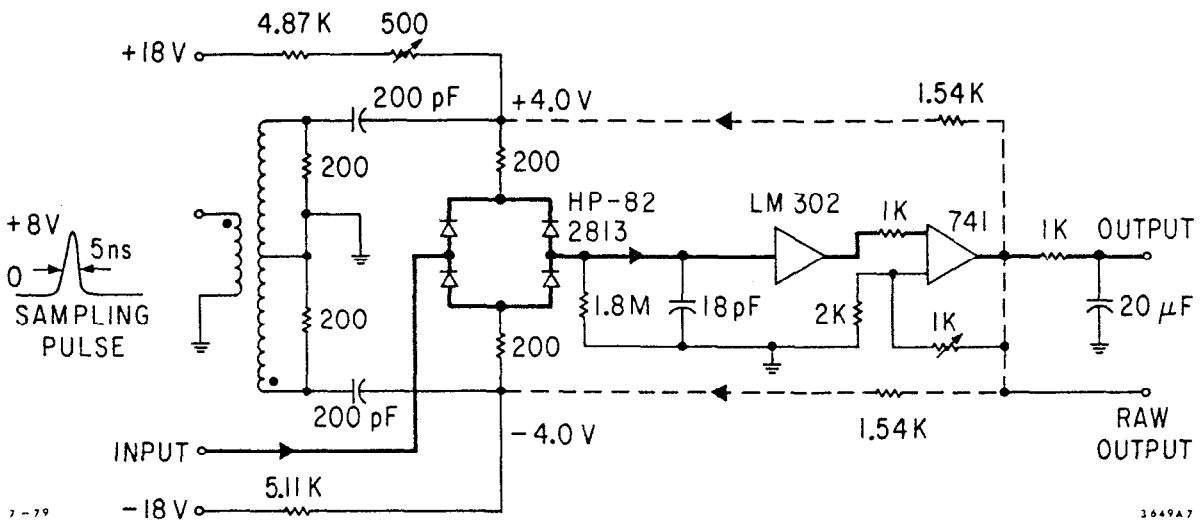
4.87 K
500
+18 V
200 pF
+4.0 V
1.54K
200
200
HP-82
2813
LM 302
1K
741
1K OUTPUT
+8V
5ns
0
SAMPLING
PULSE
200
1.8M
18pF
2K
1K
20 μF
200
200 pF
-4.0 V
1.54K
RAW
OUTPUT
INPUT
5.11 K
-18 V
7-79
3649A7

Fig. 7

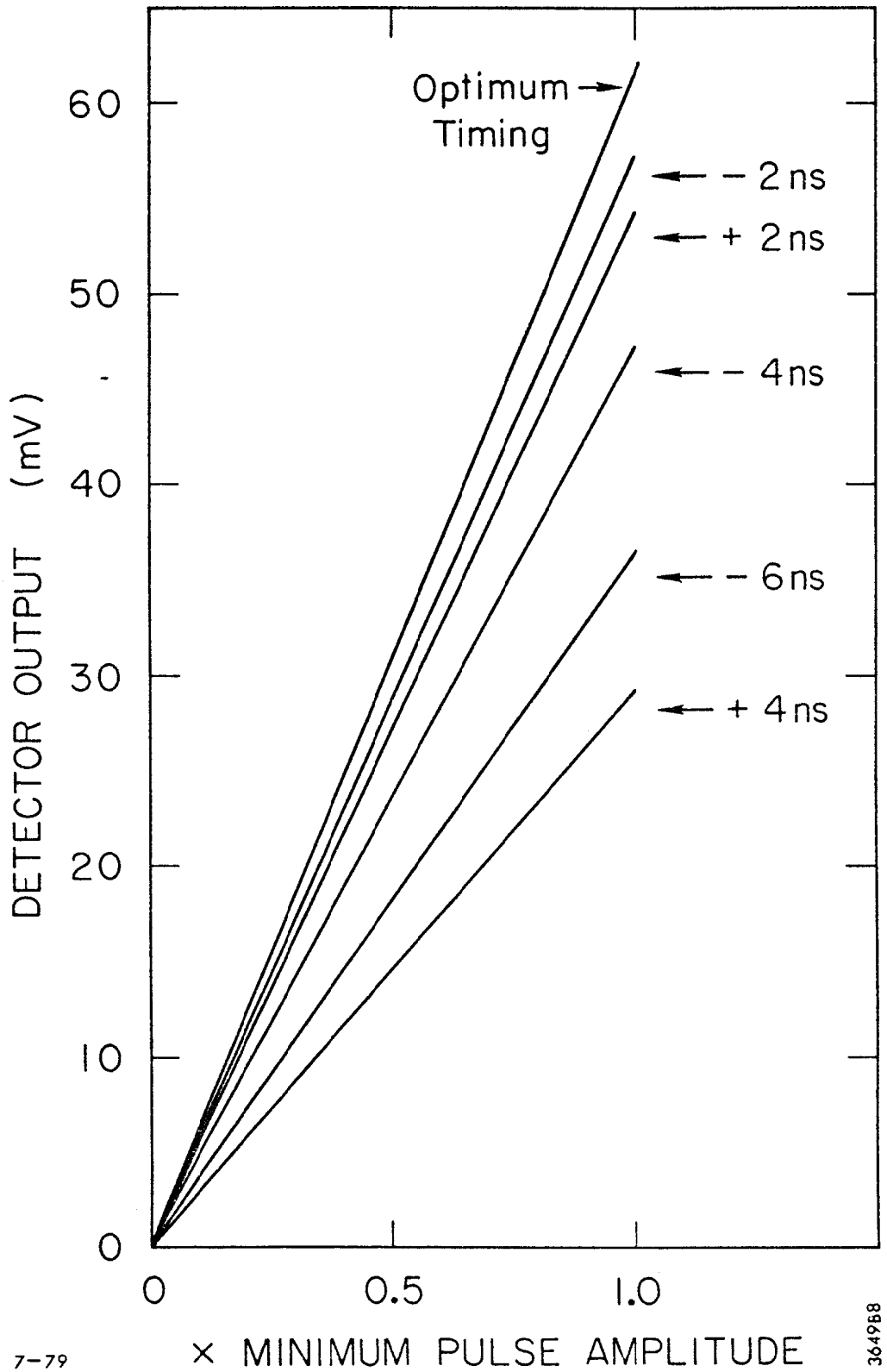
Optimum
Timing
– 2 ns
+ 2 ns
– 4 ns
– 6 ns
+ 4 ns
60
50
40
30
20
10
0
DETECTOR OUTPUT (mV)
0
0.5
1.0
× MINIMUM PULSE AMPLITUDE
7-79
364968

Fig. 8

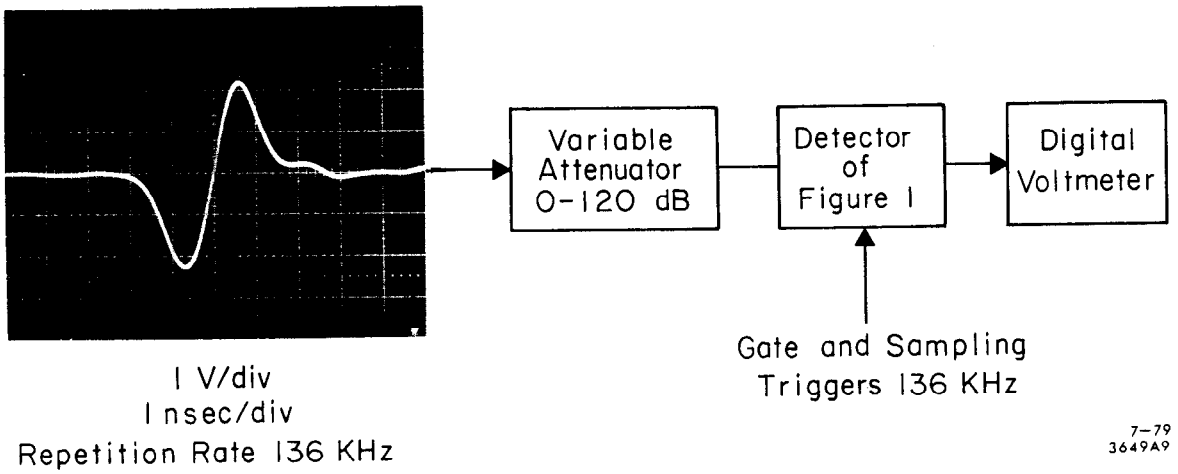
Variable
Attenuator
0-120 dB
Detector
of
Figure 1
Digital
Voltmeter
Gate and Sampling
Triggers 136 KHz
1 V/div
1 nsec/div
Repetition Rate 136 KHz
7-79
3649A9

Fig. 9

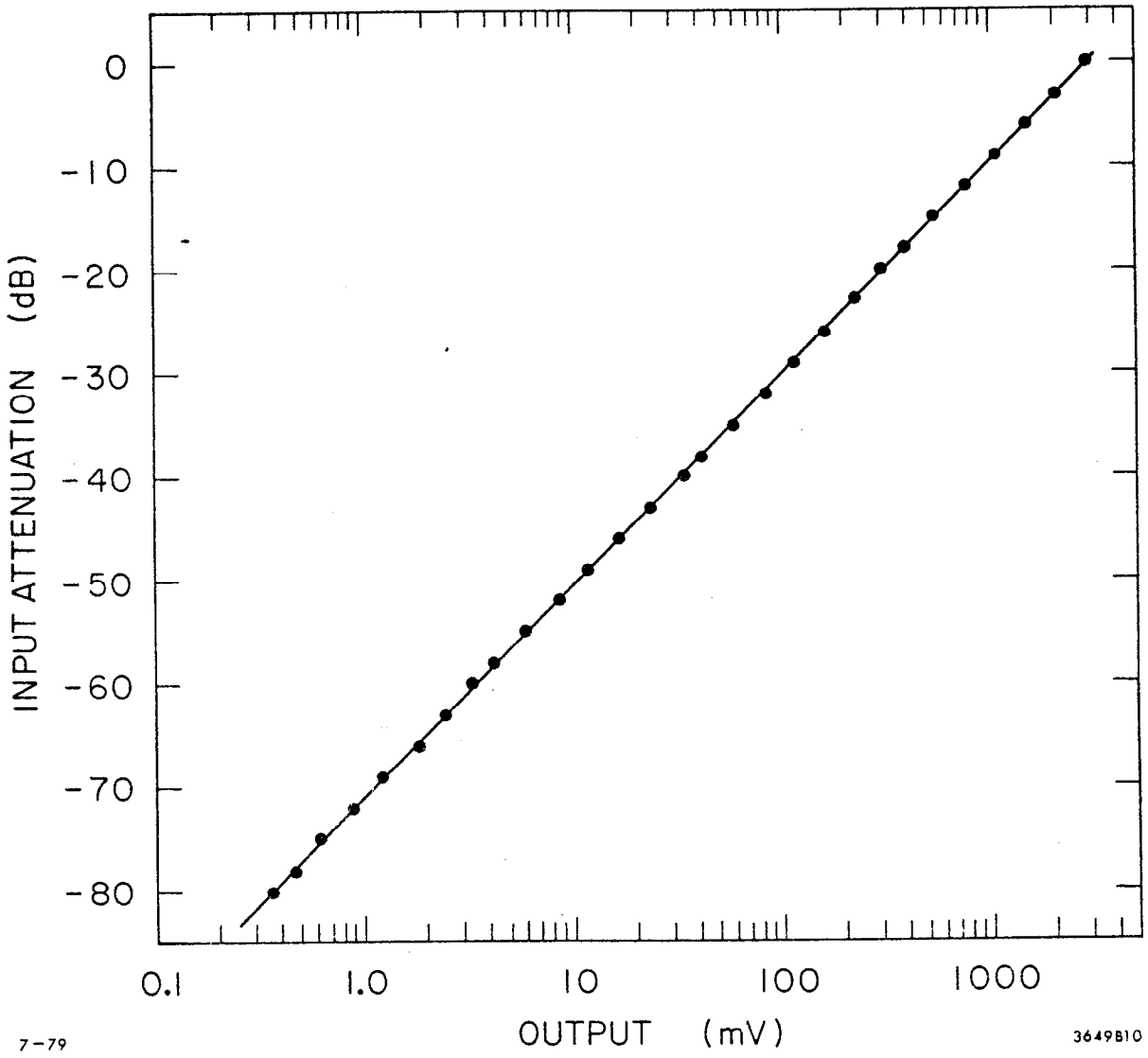
0
-10
-20
-30
-40
-50
-60
-70
-80
INPUT ATTENUATION (dB)
0.1
1.0
10
100
1000
OUTPUT (mV)
7-79
3649B10

Fig. 10